J|A|C|S
ARTICLES
Published on Web 09/11/2004

Water-Assisted Reaction Mechanism of Monozinc β-Lactamases

Matteo Dal Peraro,[†] Leticia I. Llarrull,[‡] Ursula Rothlisberger,[§] Alejandro J. Vila,[‡] and Paolo Carloni*,[†]

Contribution from the International School for Advanced Studies, SISSA-ISAS, INFM-Democritos Center, via Beirut 4, 34014 Trieste, Italy, Molecular Biology Division, IBR (Instituto de Biología Molecular y Celular de Rosario), Consejo Nacional de Investigaciones Científicas y Técnicas, and Biophysics Section, Facultad de Ciencias Bioquímicas y Farmacéuticas, Universidad Nacional de Rosario, Suipacha 531, (S2002LRK) Rosario, Argentina, and Laboratory of Computational Chemistry and Biochemistry, Institute of Molecular and Biological Chemistry, Swiss Federal Institute of Technology EPFL, CH-1015 Lausanne, Switzerland

Received April 3, 2004; E-mail: carloni@sissa.it

Abstract: Hybrid Car−Parrinello QM/MM calculations are used to investigate the reaction mechanism of hydrolysis of a common β-lactam substrate (cefotaxime) by the monozinc β-lactamase from *Bacillus cereus* (BcII). The calculations suggest a fundamental role for an active site water in the catalytic mechanism. This water molecule binds the zinc ion in the first step of the reaction, expanding the zinc coordination number and providing a proton donor adequately oriented for the second step. The free energy barriers of the two reaction steps are similar and consistent with the available experimental data. The conserved hydrogen bond network in the active site, defined by Asp120, Cys221, and His263, not only contributes to orient the nucleophile (as already proposed), but it also guides the second catalytic water molecule to the zinc ion after the substrate is bound. The hydrolysis reaction in water has a relatively high free energy barrier, which is consistent with the stability of cefotaxime in water solution. The modeled Michaelis complexes for other substrates are also characterized by the presence of an ordered water molecule in the same position, suggesting that this mechanism might be general for the hydrolysis of different β-lactam substrates.

Introduction

The increasing use of antibiotics in the clinical setting and animal feedstock imposes a high evolutionary pressure that favors selection of pathogenic microorganisms, capable of developing sophisticated strategies against drug action. The prevalent drug resistance mechanism consists in the production of β-lactamases, i.e., enzymes that catalyze the hydrolysis of the β-lactam amide moiety to produce the corresponding β-amino acid devoid of antibacterial activity.[1−4]

Clinically useful inhibitors have been successfully designed for most of these enzymes, except for metallo β-lactamases (MBLs), which are spreading among pathogenic bacteria at a steadily increasing rate.[5−7] MBLs may be active with one or two metal ions in the active site.[5−7] Whereas the enzymatic mechanism of the dizinc MBL from *Bacteroides fragilis* has been dissected in detail,[8−10] that of the monozinc species is still subject of debate.[11−14] The general sketch of the mechanism involves the nucleophilic attack of the zinc-bound hydroxide to the β-lactam carbonyl group (Step 1, Scheme 1), followed by the scission of the β-lactam C−N bond, assisted by protonation of the nitrogen atom (Step 2).[11−19] No consensus has been reached on the identity of the proton donor in Step 2:

[†] International School for Advanced School, SISSA-ISAS, INFM-Democritos Center.

[‡] Molecular Biology Division, IBR (Instituto de Biología Molecular y Celular de Rosario), Consejo Nacional de Investigaciones Científicas y Técnicas, and Biophysics Section, Facultad de Ciencias Bioquímicas y Farmacéuticas, Universidad Nacional de Rosario.

[§] Laboratory of Computational Chemistry and Biochemistry, Institute of Molecular and Biological Chemistry, Swiss Federal Institute of Technology EPFL.

(1) Frère, J. M. *Mol. Microbiol.* **1995**, *16*, 385−395.
(2) Bush, K.; Jacoby, G. A.; Medeiros, A. A. *Antimicrob. Agents Chemother.* **1995**, *39*, 1211−1233.
(3) Livermore, D. M. *Curr. Opin. Investig. Drugs* **2002**, *3*, 218−24.
(4) Nordmann, P.; Poirel, L. *Clin. Microbiol. Infect.* **2002**, *8*, 321−31.
(5) Cricco, J. A.; Vila, A. J. *Curr. Pharm. Design* **1999**, *5*, 915−927.
(6) Cricco, J. A.; Orellano, E. G.; Rasia, R. M.; Ceccarelli, E. A.; Vila, A. J. *Coord. Chem. Rev.* **1999**, *190−192*, 519−535.
(7) Wang, Z.; Fast, W.; Valentine, A. M.; Benkovic, S. J. *Curr. Opin. Chem. Biol.* **1999**, *3*, 614−622.
(8) Wang, Z.; Benkovic, S. J. *J. Biol. Chem.* **1998**, *273*, 22 402−22 408.
(9) Wang, Z.; Fast, W.; Benkovic, S. J. *Biochemistry* **1999**, *38*, 10 013−10 023.
(10) Yanchak, M. P.; Taylor, R. A.; Crowder, M. W. *Biochemistry* **2000**, *39*, 11 330−11 339.
(11) Bounaga, S.; Laws, A. P.; Galleni, M.; Page, M. I. *Biochem. J.* **1998**, *331*, 703−711.
(12) Suarez, D.; Merz, K. M., Jr. *J. Am. Chem. Soc.* **2001**, *123*, 3759−3770.
(13) Diaz, N.; Suarez, D.; Merz, K. M., Jr. *J Am. Chem Soc.* **2001**, *123*, 9867−9879.
(14) Olsen, L.; Antony, J.; Ryde, U.; Adolph, H.-W.; Hemmingsen, L. *J. Phys. Chem. B* **2003**, *107*, 2366−2375.
(15) Carfi, A.; Pares, S.; Duee, E.; Galleni, M.; Duez, C.; Frère, J. M.; Dideberg, O. *EMBO J.* **1995**, *14*, 4914−4921.
(16) Fabiane, S. M.; Sohi, M. K.; Wan, T.; Payne, D. J.; Bateson, J. H.; Mitchell, T.; Sutton, B. J. *Biochemistry* **1998**, *37*, 12 404−12 411.
(17) Dal Peraro, M.; Vila, A. J.; Carloni, P. *J Biol. Inorg. Chem* **2002**, *7*, 704−712.
(18) Dal Peraro, M.; Vila, A. J.; Carloni, P. *Inorg. Chem.* **2002**, *42*, 4245−4247.

Scheme 1

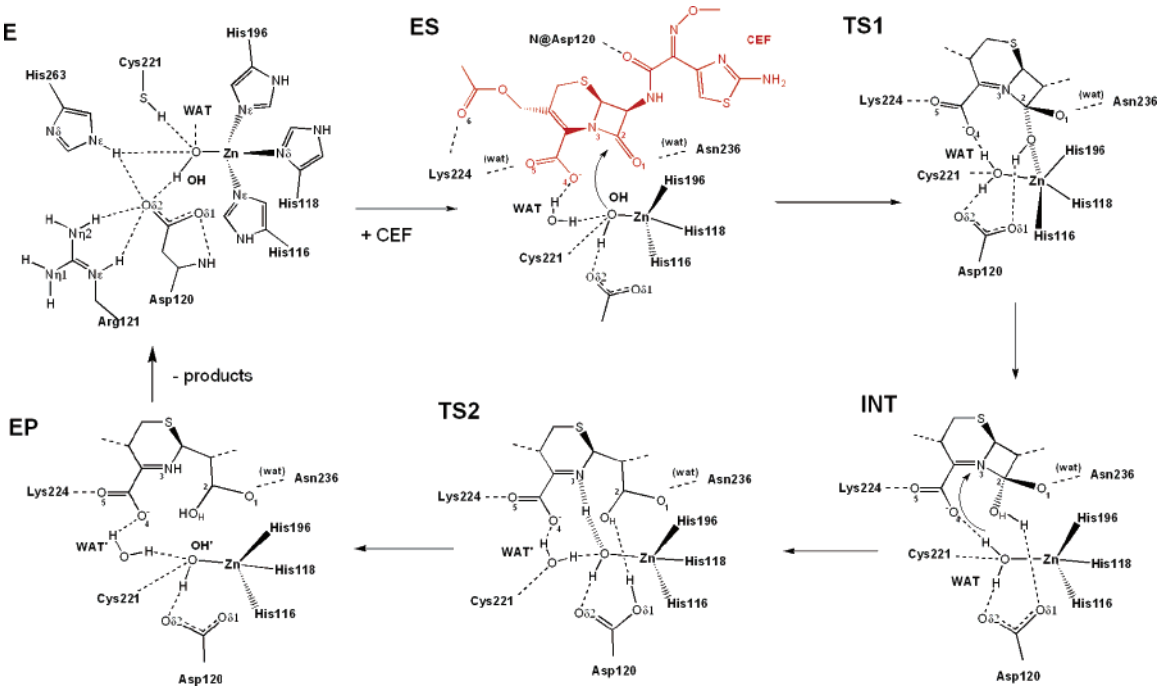

Asp120, His263, Cys221 or a solvent molecule have been postulated as putative candidates.[11−14]

Here, we report a detailed theoretical study of the mechanism of hydrolysis of a common antibiotic, cefotaxime (CEF, Scheme 1 in red, Figure 1), by the monozinc β-lactamase from *Bacillus cereus* (BcII). BcII is active both in the mono or dizinc forms, but the monozinc derivative is thought to be the active species in vivo.[20−22] BcII is one of the most widely studied MBLs and its study may be extrapolated to the MBL from *Bacillus anthracis*,[23] which has 92% sequence identity with BcII. Comparison is made with the corresponding reaction in water. Our approach is the hybrid Car−Parrinello MD/MM simulation, which has already been shown to describe the electronic structure of a dinuclear zinc designed protein.[24] Thus, it is expected to be well suited to study this system.

The quantum molecular modeling presented here provides a novel mechanism, in which an ordered water molecule buried in the active site plays a direct and crucial role in catalysis by binding the metal ion as the reaction proceeds. This is a previously unrecognized feature in catalysis by monozinc MBLs that fills several gaps in the proposed schemes and might be general for the hydrolysis of BcII substrates.

Computational Details

Enzymatic Hydrolysis. The calculations were based on the BcII−CEF structure[25] in aqueous solution, as obtained after ∼2.2 ns of MD simulations. In this work, (i) the protonation state of the residues at the active site at physiological pH was that determined by extensive DFT calculations on large models of the BcII active site (Scheme 1 and Figure 1).[17] (ii) The protonation state of all the other titratable residues was also assumed according to physiological pH conditions, as discussed in ref 25. Thus, the active site His residues His116, His118, His196, and His263 were protonated on Nδ, Nϵ, Nδ, and Nϵ atoms, respectively (Figure 1), whereas other His protonation states were assigned based on visual inspection of their putative H-bond patterns: His55 (Nϵ), His136 (Nδ, Nϵ), and His285 (Nϵ). Asp and Glu groups were assumed to be ionized. (iii) The substrate cefotaxime (Scheme 1) was docked into the active site using the program Dock[26] with the electrostatic and van der Waals parameters of ref 25, and a 64^3 points spatial grid, with 0.25 Å spacing, centered on the zinc ion.[25] (iv) Water molecules solvating BcII were explicitly treated.

The complex was partitioned in a QM region, which included the reactive center (i.e., CEF, the zinc ion and its coordination polyhedron, Figure 1 in Supporting Information), and a MM region composed by the rest of the protein immersed in a water box (∼38 000 atoms).

The MM part was treated with the AMBER force field;[27] the PME method was used to evaluate long-range electrostatic interactions.[28] A cutoff of 12 Å was used to account for the van der Waals interactions and the short range, real part contribution to the PME. The QM part was treated using density functional theory-based molecular dynamics simulations, following the approach of Car and Parrinello,[29] which has been shown to describe accurately a variety of enzymatic systems,[30]

(19) Page, M. I. *The chemistry of β-lactams*; Blackie Academic & Professional: London, 1992.
(20) Paul-Soto, R.; Bauer, R.; Frère, J. M.; Galleni, M.; Meyer-Klaucke, W.; Nolting, H.; Rossolini, G. M.; de Seny, D.; Hernandez-Valladares, M.; Zeppezauer, M.; et al. *J. Biol. Chem.* **1999**, *274*, 13 242−13 249.
(21) Orellano, E. G.; Girardini, J. E.; Cricco, J. A.; Ceccarelli, E. A.; Vila, A. J. *Biochemistry* **1998**, *37*, 10 173−10 180.
(22) Wommer, S.; Rival, S.; Heinz, U.; Galleni, M.; Frère, J. M.; Franceschini, N.; Amicosante, G.; Rasmussen, B.; Bauer, R.; Adolph, H. W. *J. Biol. Chem.* **2002**, *277*, 24 142−24 147.
(23) Materon, I.; Queenan, A.; Koehler, T.; Bush, K.; Palzkill, T. *Antimicrob Agents Chemother* **2003**, *47*, 2040−2042.
(24) Magistrato, A.; DeGrado, W. F.; Laio, A.; Rothlisberger, U.; VandeVondele, J.; Klein, M. L. *J. Phys. Chem. B* **2003**, *107*, 4182−4188.
(25) Dal Peraro, M.; Vila, A. J.; Carloni, P. *Proteins* **2004**, *54*, 412−423.
(26) Ewing, T.; Kuntz, I. *J. Comp. Chem.* **1997**, *18*, 1175−1189.
(27) Case, D. A.; Pearlman, D. A.; Caldwell, J. W.; Cheatham, T. E., III; Ross, W. S.; Simmerling, C. L.; Darden, T. A.; Merz, K. M.; Stanton, R. V.; Cheng, A. L.; et al. *AMBER 6*; University of California: San Francisco, 1999.
(28) Darden, T. A.;York, D. *J. Chem. Phys.* **1993**, *98*, 10 089−10 094.
(29) Car, R.; Parrinello, M. *Phys. Rev. Lett.* **1985**, *55*, 2471−2474.
(30) Carloni, P.; Rothlisberger, U.; Parrinello, M. *Acc. Chem. Res.* **2002**, *35*, 455−464.

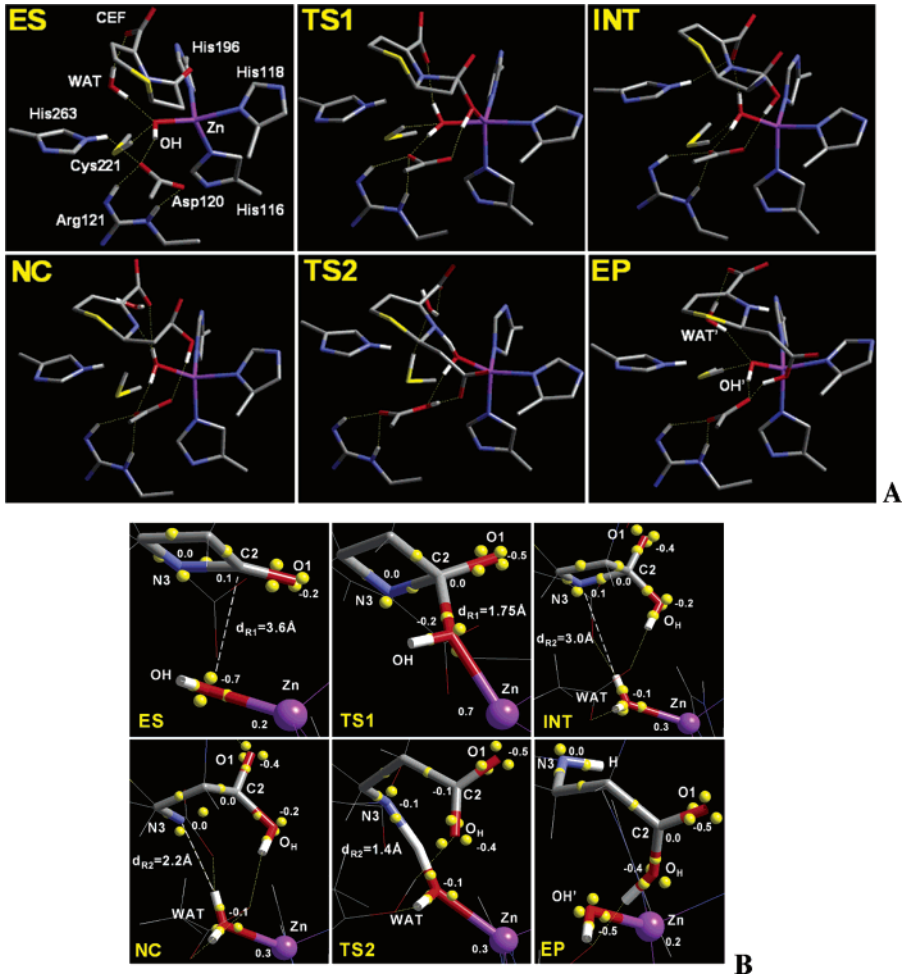

Figure 1. 3D (A) and electronic (B) structures of species relevant for the catalytic cycle. In B, the Boys orbitals (BO's), which can be associated to chemical bonds and electronic lone pairs,[43] are depicted as yellow spheres.

including Zn-based enzymes.[24,31] The valence electrons were described by a plane wave basis set up to a cutoff of 70 Ry, which is not affected by basis set superposition errors.[32] The interactions between valence electrons and ionic cores were described with norm-conserving Martins−Troullier[33] pseudopotentials. The BLYP[34,35] exchange-correlation functional was used. This functional, along with planewaves basis set, has demonstrated to correctly describe aqueous and biological systems.[30,36] Notice that the use of popular B3LYP functional[34,35] along with in plane-wave based calculations is computationally highly inefficient.[32] Car−Parrinello molecular dynamics[29] simulations were carried out with a time step of 0.14 fs and a fictitious electron mass of 900 au; constant temperature simulations were achieved by coupling the system with a Nosé−Hoover[37,38] thermostat at 500 cm^{-1} frequency. The interactions between the MM and QM regions were treated as in ref 39. The free energies of activation were evaluated with the method of thermodynamics integration,[40] by numerical integration of the dynamically averaged force profile along three constrained reaction coordinates, namely $d_{R1} = d$(O@OH−C2@CEF), $d_{R2} = d$(H@WAT−N3@CEF), and $d_{R3} = d$(H−Oδ1@Asp120−O_H). For each point along d_R, ∼0.5 ps were used for thermalization, and ∼1 ps for averaging the force on the constraint and for calculating the errors on the forces. Hysteresis effects affecting the free energy profile were estimated by applying the constrained dynamics described below backward along the same reaction coordinates paths.[41]

The protocol for QM/MM simulation was as follows: (i) ∼0.1 ps of dynamics of the MM region with QM part frozen, followed by ∼3 ps of dynamics for the entire system; (ii) constrained dynamics using d_{R1} as the reaction coordinate, from 3.6 Å (ES structure) until 1.4 Å (INT structure, Scheme 1 and Figure 1), is performed in 12 steps; (iii) ∼2 ps dynamics of INT; (iv) constrained dynamics assuming d_{R2} as the reaction coordinate (Figure 1), from 3.0 Å until 1.4 Å (TS2 structure); (iv) ∼2 ps of dynamics on the entire system; and (v) constrained dynamics assuming d_{R3} as the reaction coordinate.

D-RESP atomic partial charges[42] in the QM regions, which reproduce the quantum electrostatic potential polarized by the

(31) Rothlisberger, U. *ACS Sym. Ser.* **1998**, *712*, 264−231.
(32) Marx, D.; Hutter, J. *Mod. Methods Algorithms Quantum Chem.* **2000**, *1*, 301−449.
(33) Troullier, N.; Martins, J. L. *Phys. Rev. B* **1991**, *43*, 1943−2006.
(34) Becke, A. D. *Phys. Rev. A* **1988**, *38*, 3098−3100.
(35) Lee, C.; Yang, W.; Parr, R. G. *Phys. Rev. B* **1988**, *37*, 785−789.
(36) Silvestrelli, P. L.; Parrinello, M. *Phys. Rev. Lett.* **1999**, *82*, 3308−3311.
(37) Nose′, S. J. *J. Chem. Phys.* **1984**, *81*, 511−519.
(38) Hoover, W. G. *Phys. Rev. A* **1985**, *31*, 1695−1697.
(39) Laio, A.; vandeVondele, J.; Roethlisberger, U. *J. Chem. Phys.* **2002**, *116*, 6941−6947.
(40) Ciccotti, G.; Ferrario, M.; Hynes, J. T.; Kapral, R. *Chem. Phys.* **1989**, *129*, 241−251.
(41) Sulpizi, M.; Laio, A.; VandeVondele, J.; Cattaneo, A.; Rothlisberger, U.; Carloni, P. *Proteins* **2003**, *52*, 212−224.
(42) Laio, A.; VandeVondele, J.; Rothlisberger, U. *J. Phys. Chem. B* **2002**, *106*, 7300−7307.

Table 1. Selected Bond Lengths, Angles, and Planarity of the Species in Scheme 1

	ES	TS1	INT	TS2	EP
O1−C2	1.22(1)	1.22(2)	1.33(3)	1.26(1)	1.27(1)
O1−Zn	4.14(45)	3.72(23)	5.24(13)	6.00(1)	6.02(9)
C2−N3	1.39(2)	1.53(4)	1.59(3)	3.25(3)	3.35(6)
C2−O@OH (d_{R1})	3.63(27)	1.75	1.44(4)	1.27(1)	1.27(1)
N3−H@WAT (d_{R2})	−	3.25(24)	3.10(10)	1.40	1.05(6)
Zn−Nδ@His116	2.15(6)	2.16(9)	2.09(5)	2.18(5)	2.15(6)
Zn−Nϵ@His118	2.10(5)	2.17(8)	2.06(5)	2.06(4)	2.09(6)
Zn−Nδ@His196	2.13(6)	2.08(5)	2.06(4)	2.05(5)	2.08(5)
Zn−O@OH	1.92(3)	2.15(11)	2.3/4.5	4.62(9)	−
Zn−O@WAT	−	2.03(7)	2.10(9)	2.07(4)	1.94(2)
N3 angles	94(2)	92(3)	95(2)	120(3)	114(3)
	137(3)	124(2)	125(3)	104(4)	111(3)
	125(3)	123(2)	127(4)	118(3)	124(4)
N3 planarity	13(6)	29(4)	25(5)	−30(2)	−25(4)
C2 planarity	1(1)	21(1)	26(2)	3(2)	2(1)
Zn planarity	28(4)	4(3)	31(2)	30(3)	30(3)

protein−water electric field, were calculated along the reaction, as well as Boys' orbitals, which can be associated to electron lone pairs and localized chemical bonds.[43] Notice that the π-electrons of the β-lactam ring are not delocalized (Figures 2 and 3 in Supporting Information (SI)), so that the localization procedure in calculating the latter is fully justified. The CPMD 3.5 with the QM/MM interface of ref 39 was used for the calculations, running on an IBM SP4 parallel computer. The VMD package[44] was used for analysis and visualization.

Hydrolysis in Aqueous Solution. As a reference, we modeled the first step of the hydrolysis of CEF in water. CEF was inserted in a water box and underwent ∼5 ns MD simulation. Subsequently, the system was partitioned in a QM region, which included CEF and its solvation sphere around the β-lactam ring (38 atoms), and a MM region, consisting of the remaining water molecules (∼3000). Constrained QM/MM simulations were carried out in which the distance between the oxygen of the catalytic water and the carbonyl carbon C2 (d_{R1}) was assumed as the reaction coordinate, and shortened from 3.2 to 1.4 Å.

Structural Models of BcII−BPC and BcII−IMI Complexes. The ES complexes of BcII with benzylpenicillin (BPC) and imipenem (IMI) were modeled as previously done for the BcII−CEF model,[25] used here for QM calculations. The BPC and IMI structures and force field parameters were taken from refs 13, 45. The substrates were docked onto the BcII X-ray structure (pdb code 3bc2) employing the program Dock,[26] with the same protocol described above and in ref 25. Approximately 2 ns MD simulations employing the AMBER force field[27] were performed on these models using the setup and analysis protocol reported for the BcII−CEF complex.[25]

Results and Discussion

The H-bond pattern of the Michaelis complex of CEF with monozinc BcII emerging from a previous classical MD study[25] is fully maintained in the QM/MM simulation (ES in Scheme 1 and Figure 1): the zinc-bound OH H-bonds to Asp120, Cys221, and an ordered water molecule (WAT). Asp120 also forms a stable salt bridge with Arg121. The solvent molecule WAT is bridging the zinc-bound OH and the CEF carboxylate group. O@OH is 3.6(3) Å far from the carbonyl C2 atom, whereas the zinc ion is at a distance of 4.2(3) Å from O1@CEF. The CEF carboxylate group interacts throughout the reaction with Lys224 by means of H-bonds mediated by water molecules. Relevant geometric parameters, hydrogen bond distances and D-RESP charges for the relevant species in the reaction are summarized in Tables 1−2 and Figure 1B.

Step 1. The reaction coordinate, d(O@OH−C2@CEF) = d_{R1}, is shortened from its initial value (3.6 Å, ES species, Scheme 1) until the sign of the constrained force changes (d = 1.75 Å, TS1 species). The rearrangement of the electron lone pairs and chemical bonds during the enzymatic reaction are described here in terms of Boys' Orbitals[43] (BO's) (Figure 1B).

When d_{R1} = 1.9 Å, the O@OH−Zn bond, identified by a BO, becomes increasingly polar. The S@Cys221 loses the H-bond interaction with O@OH, and now interacts with WAT. At d_{R1} = 1.8 Å, a key event occurs: WAT enters the first coordination sphere of the zinc ion, changing the zinc geometry from tetrahedral to trigonal bi-pyramidal (TS1 in Figure 1): WAT, His118 and His196 lie in the equatorial plane, whereas His116 and OH are the apical ligands. This rearrangement affects the H-bond pattern in the active site: now WAT interacts with S@Cys221, Oδ2@Asp120 and O4@CEF, whereas the attacking OH H-bonds to the Oδ1@Asp120, and His263 H-bonds to Oδ2@Asp120 and O4@CEF (Scheme 1, Figure 1 and Table 2). The C2 atom acquires an sp^3 hybridization (Figure 1). At d_{R1} = 1.7 Å, the forces on the constraint change sign, suggesting that the transition state has been reached (TS1), and the C2−O1 bond adopts a single bond character (Figure 1B, Figure 2 in SI). The Zn−OH and N3−C2 bonds weaken (d = 2.1(1) Å and 1.5(1) Å, respectively), and become very polar, as suggested by the displacement of the BO's (Figure 1B), as well as by the increase of the charges at O@OH and at the zinc ion, along with a decrease of the charge at O1@CEF (Figure 1B).

After TS1, d_{R1} is further decreased from 1.7 to 1.4 Å, where the average constraint force is essentially zero, suggesting that the C2@CEF−O@OH bond is fully formed. The Zn−O bond fluctuates around a rather large value (2.3(2) Å). Upon removal of the constraint, the reaction intermediate (INT) is formed: the Zn−OH bond spontaneously breaks (d = 4.5 Å), thus restoring a distorted tetrahedral polyhedron for the zinc ion, with WAT, His116, His118, and His196 as ligands. As expected, WAT oxygen is less negative than that of OH (Figure 1B). The zinc

(43) Marzari, N.; Vanderbilt, D. *Phys. Rev. B* **1997**, *56*, 12847−12865.
(44) Humphrey, W.; Dalke, A.; Schulten, K. *J. Mol. Graphics* **1996**, *14*, 33−38.
(45) Suarez, D.; Dimas, N.; Merz, K. M., Jr. *J. Comput. Chem.* **2002**, *23*, 1587−1600.

Table 2. Selected H-Bond Distances (Å) for the Species in Scheme 1, as Obtained from the QM/MM Calculations

H-bond distances	ES	TS1	INT	TS2	EP
OH−H@WAT	1.94(18)				
OH′−H@WAT′					2.30(71)
H@OH···Oδ2@Asp120	1.72(15)				
H@OH···Oδ1@Asp120		1.54(10)	1.87(13)	1.02(1)	2.26(21)
H@WAT···Oδ2@Asp120		1.82(10)	1.75(12)	1.89(4)	
H@OH′···Oδ2@Asp120					1.83(3)
O@OH···H−S@Cys221	1.97(14)				
O@WAT··· H−S@Cys221		2.26(53)	2.10(15)	5.05(46)	
O@OH′··· H−S@Cys221					2.34(38)
O@WAT′··· H−S@Cys221				3.20(9)	3.73(81)
O@OH···H−Nϵ@His263	2.47(17)				
O@WAT···H−Nϵ@His263		3.20(22)	3.04(20)	3.02(6)	
O@OH′···H−Nϵ@His263					3.20(33)
O4···H_C@WAT	1.85(12)	1.82(10)	1.96(13)	3.27(16)	1.98(30)
Oδ2@Asp120···H−Nη1@Arg121	1.85(10)	1.91(13)	1.91(11)	1.92(12)	2.09(17)
Oδ2@Asp120···H−Nϵ@Arg121	2.00(19)	1.95(16)	1.95(13)	2.07(9)	1.96(13)
Oδ2@Asp120···H−Nϵ@His263	2.30(28)	2.32(32)	2.53(54)	3.14(14)	3.29(25)
O7···H−N@Asp120	2.03(13)	3.46(37)	3.58(36)	5.54(16)	2.09(16)

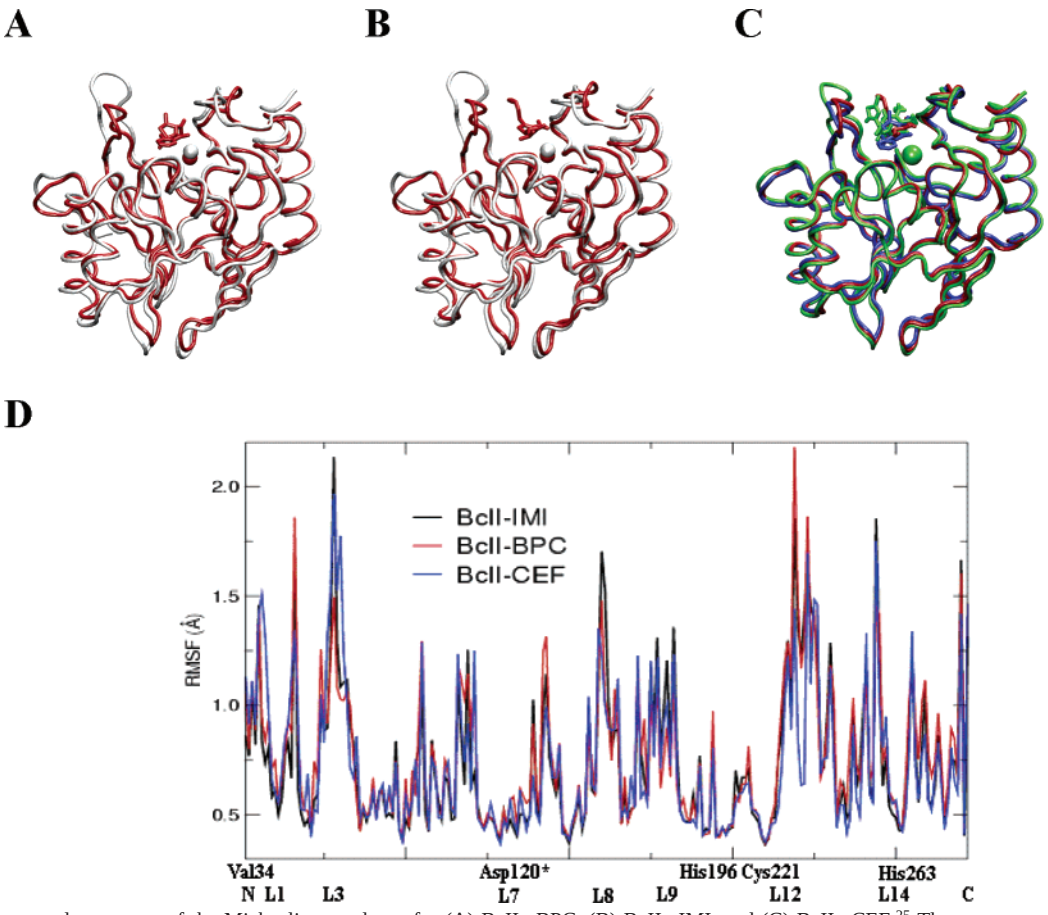

Figure 2. MD averaged structures of the Michaelis complexes for (A) BcII−BPC, (B) BcII−IMI, and (C) BcII−CEF.[25] The structures are overlaid with the X-ray structure of free BcII (in gray). The zinc ions are represented as spheres, and the docked substrates are depicted as sticks. (D) Root-mean-square fluctuations of BcII−CEF, BcII−BPC and BcII−IMI MD structures (active site residues and loop regions are indicated in abscissa as in ref 25).

charge changes during the reaction in a nontrivial manner, being affected possibly by several factors, including the distance between the metal ion and its ligands, the coordination number and the presence of either a water molecule or an OH group binding to the Zn. The metal-bound WAT moiety H-bonds to Oδ2@Asp120 and to the O4@CEF carboxylate moiety. The C2−N3 bond is significantly weakened, fluctuating around 1.6-(1) Å, and becoming much more polar than in the ES complex (Tables 1, 2, Figure 1B).

Step 2. In the initial structural model for this step (INT, Figure 1), WAT H-bonds to Oδ2@Asp120, whereas Oδ1@Asp120 H-bonds to CEF and Arg121. To investigate the scission of the C2−N3 bond, we assume that this event is assisted by protonation of the β-lactam N3 atom.[15] It has been suggested that this proton could be delivered by Cys221, Asp120, His263, or by a water molecule.[11−14] However, Asp 120 is deprotonated. His263 is unlikely to donate its polar hydrogen since it is located rather far from N3 (∼4 Å), and it is not well oriented

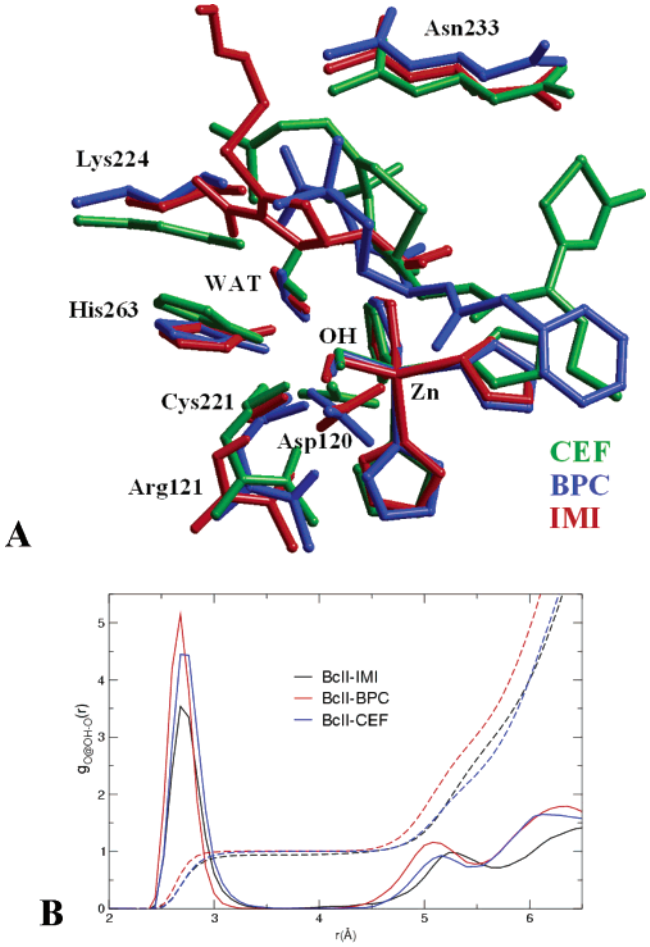

Figure 3. (A) Comparison between BcII−CEF, BcII−BPC, and BcII−IMI MD structures after ∼2 ns. (B) O@OH-water oxygen g(r)'s for the three MD simulations.

(H@His263···N3−C2@CEF ≈ 140°). In addition, a neutral imidazole is expected to be less acid than a zinc-bound water. The proposal of His263 as the proton donor in Step 2 relies in the assumption that the imidazole is positively charged.[12,13] However, DFT calculations on extended models of the active site predict that His263 is neutral in the resting state,[17] allowing us to discard this hypothesis. Cys221, on its turn, is even farther from N3 (∼6 Å). Instead, the zinc-bound WAT, which is the only water accessible to N3, is very well suited to act as a proton donor based on its distance (and orientation) to the N3 atom (∼3.3 Å, H@WAT···N3−C2@CEF ≈ 90°) and on its low pK_a.[17,46,47] Thus, d(H@WAT−N3@CEF) = d_{R2} is chosen as the reaction coordinate. d_{R2} is shortened from its initial value (3.3 Å) to 1.4 Å, where the forces approach zero. The tetrahedral coordination of the zinc ion and its charge are fully preserved during this step (Figure 1, Tables 1−2).

At d_{R2} = 2.25 Å, the C2−N3 bond breaks, and the N3 atom now has an additional lone pair, and it is not yet protonated (NC, Figure 1B and Figure 3 in SI). The recently formed O1−C2−OH carboxylate moiety is able to transfer its proton to Oδ1@Asp120. At d_{R2} = 1.4 Å, TS2 is reached (Figure 1B): one of the two N3 lone pairs rearranges to form the N3−H bond. Consistently, the H−O@WAT bond is elongated to 1.1 Å, and the Zn−O@WAT bond distance is shortened (Table 1). WAT loses its H-bond with Cys221, which in turn drives another water molecule (WAT′) from the bulk solvent to the active site by means of a H-bond interaction (Figure 1A, Table 2).

Upon removal of the constraint, the N3−H bond is completely formed, and the WAT O−H bond breaks, regenerating a hydroxyl moiety (OH′) bound to the zinc ion, i.e., the nucleophile. In fact, the Zn−O@WAT bond length (d = 1.9(1) Å) is consistent with a zinc-bound OH (Table 1). Cys221 H-bonds to the newly formed zinc-bound hydroxide (OH′) (Table 2), whereas WAT′ is engaged in a H-bond network similar to that involving WAT in the ES species (Scheme 1, Table 2). Finally, Asp120 can be easily deprotonated (see below) to yield EP.

Free Energy Profile. The free energy of Step 1, $\Delta F^{\ddagger}_1$, turns out to be 18.5(2.0) kcal/mol, whereas the free energy of Step 2, $\Delta F^{\ddagger}_2$, is larger (21.0(2.0) kcal/mol). However, because of the approximations herein employed (most notably the BLYP approximation,[34,35] the limited sampling of configurations, and the force-field treatment of the protein frame), we estimate that the errors in these values prevent us from identifying the slowest step in the reaction. It should be noticed that the overall barriers are in fair agreement with the experimental and theoretical data estimated for the hydrolysis of similar β-lactams.[13,14,48]

The free energy associated with the proton transfer from Asp120 to CEF O1−C2−O_H carboxylate (3(1) kcal/mol) is much smaller than those for Step 1 and Step 2, allowing us to discard this chemical event as rate-limiting.

Comparison with the Corresponding Reaction in Water. In the first step of the simulation of the water-mediated hydrolysis of CEF, TS1 is formed at much shorter distances (d_{R1} = 1.5 Å), and the hydrolytic water loses a proton during the nucleophilic attack (see SI). The calculated $\Delta F^{\ddagger}_1$ is much larger than in the enzyme catalyzed reaction (48(3) kcal/mol), possibly due to the huge free energy cost associated with the cleavage of the H−O bond relative to that of the Zn−O bond in the enzyme (see SI).

Role of WAT and Extension of the Mechanism to Other Substrates. Our calculations predict a water-assisted proton transfer in the enzymatic mechanism not suggested before for these enzymes. The involved water molecule WAT, initially sandwiched between the metal center and the substrate as revealed by MD study[25] (Figure 1), coordinates the zinc ion in the first transition state TS1, guided by the H-bond interactions with Cys221 and Asp120, giving rise to a pentacoordinated species. This event assists the reaction, since the cleavage of the Zn−OH bond is counterbalanced by the formation of a Zn−WAT bond. This fundamental feature is facilitated in BcII by the existence of a relatively open active site that allows for the presence of WAT in the zinc coordination sphere in the enzyme/CEF complex, as emerged from our previous MD simulation.[25] Thus, the zinc ion and the surrounding hydrogen bond network in the active site may be depicted as a machinery conveying water molecules to act as nucleophiles (Step 1, Figure 1) and proton donors (Step 2). Binding of this water molecule to the zinc ion is crucial for (i) favoring the proton transfer, by lowering WAT pK_a, and (ii) adequately orienting WAT for Step 2. This arrangement facilitates both the nucleophilic attack and the N3 protonation to occur at the same face of the substrate.

(46) Merz, K. M., Jr. *J. Mol. Biol.* **1990**, *214*, 799−802.
(47) Rasia, R. M.; Vila, A. J. *Biochemistry* **2002**, *41*, 1853−1860.
(48) Bicknell, R.; Waley, S. G. *Biochem. J.* **1985**, *231*, 83−88.

This is contrary to the theory of stereoelectronic effects, which predicts that the nucleophilic attack and the nitrogen protonation in amide hydrolysis should be antiperiplanar.[49] However, the butterfly shape of β-lactam antibiotics favors both chemical events to occur at the less hindered α face of the substrate.[19]

Zinc(II) is a d^{10} transition metal ion, with a flexible coordination geometry, based on its null ligand field stabilization energy and its fast ligand exchange features.[50] Many crystal structures have accounted for changes in the metal coordination sphere of zinc enzymes complexes with inhibitors, substrates or transition state analogues.[51] In particular, the direct involvement of an additional water molecule during turnover has been recently characterized in detail for the zinc enzyme alcohol dehydrogenase.[52] However, in that case, water binds to the metal ion *before* substrate binding and not during the formation of the transition state. The experimental and the theoretical characterization of this feature in metallohydrolases have been thwarted by two main reasons. First, it is very difficult to follow the zinc active site reactivity experimentally, since zinc is silent to most spectroscopic methods. Second, the studies of these enzymes have been based on X-ray[11] or gas-phase structures,[12,14] which lack this ordered water molecule.[25]

To analyze whether the water-assisted mechanism might be a general feature of β-lactam hydrolysis, we have performed AMBER force field[27] based MD simulations in the ns scale of adducts with two other β-lactams, which, together with CEF, are representative of three groups of clinically used β-lactam antibiotics. These are benzylpenicillin (BPC) and imipenem (IMI) from penicillins and carbapenems family, respectively (Figures 2,3 and Supporting Information). The location of WAT and its H-bond pattern turn out to be conserved in the three enzyme−substrate complexes, providing an *identical* degree of solvation for the zinc ion and the nucleophilic OH (Figure 3B). Both BPC and IMI are very stable in the site, with small root-mean-square deviations (2.5(1) and 2.2(2) Å, respectively), giving productive Michaelis complex adducts, as indicated by the β-lactam carbonyl/zinc-bound hydroxide distances (3.6(4) Å for BPC, 3.9(5) Å for IMI, compared to 3.6 Å for CEF), and by the optimal reciprocal orientation of the nucleophilic OH and the β-lactam carbonyl group (Figure 3A and Supporting Information). These data correlate well with pre-steady-state binding data, that reveal a high k_{off} value for BPC binding, a lower k_{off} value for cephalosporins, and a stable, nonproductive BcII−IMI complex that rearranges to yield a productive adduct.[53]

On the basis of these findings, we feel confident to propose that a similar mechanism, involving a water molecule as a proton donor in Step 2, may be operative in the hydrolysis of the three types of β-lactams. These substrates possess a β-lactam bicyclic structure with a carboxylate group that is fundamental for binding, despite adopting a slightly different orientation in the Michaelis complexes (Figure 3A, Tables 1,2 in SI). This could also explain the fact that monobactams, which lack a bicyclic core and the carboxylate moiety, are not hydrolyzed by BcII. The β-lactams' carboxylate group,[54] besides being involved in substrate binding in B1 MBLs, is a key structural determinant for the positioning of WAT.

Upon TS2 formation, another water molecule (WAT′) from the bulk is guided to the cleavage site by Cys221, which is properly aligned along a channel between the metal center and the substrate. WAT′ might then be involved in the next catalytic cycle. The crystal structure of monozinc Cys221Ser BcII reveals a disrupted H-bond network in the active site, which, in line with these predictions, could be the cause of the observed decrease in activity.[55]

Comparison with Other Proposed Mechanisms. The herein proposed mechanism differs from others previously proposed in some central features. In the first step, the authors of refs 13 and 14 have proposed that the β-lactam carbonyl acts as a fifth ligand of zinc in Step 1. Instead, in our simulation, the zinc ion expands its coordination geometry by binding WAT and the carbonyl group remains relatively far from the zinc ion (3.7(2) Å, Table 1). Simple gas-phase model calculations performed here suggest that inclusion of a zinc-bound water at TS1 stabilizes the structure by ∼10 kcal/mol, and yields a zinc−carbonyl distance larger than in a model without a coordinated water molecule (see SI). Overall, these evidences suggest that WAT is able to stabilize TS1 much better than the β-lactam carbonyl, since it is a much more flexible ligand than the substrate.

In the second step, in our mechanism, the binding of WAT to the zinc ion clearly leaves this water molecule as the sterically and energetically favored proton donor to the β-lactam nitrogen, instead of what was proposed in other mechanisms, which involve Asp120[11] or His263[12,13] as proton donors. Our proposal differs also from the hypothesis that a water molecule could be the proton source,[14] in fact in our model WAT is directly bound to the metal ion and therefore is a much better proton donor. Our mechanism, as well as those already proposed, can only be validated when more mutational, kinetic, spectroscopic, and/or crystallographic studies are available.

Role of Active Site Residues in the Reaction. Our calculations provide information on the role of conserved residues at the active site, which have been shown to be involved in catalysis by mutagenesis experiments: (i) Asp120, which is conserved in all MBLs[56] and whose mutation impairs the enzyme activity (unpublished results from our laboratory),[57] plays a fundamental role in the reaction not only by orienting the attacking OH[47] but also by steering WAT toward the metal ion and by assisting the zinc site reorganization upon the nucleophilic attack. Asp120 is also involved in the proton transfer in Step 2 through a proton relay mechanism. In this model, Asp120 accepts a proton from a carboxylate moiety that is formed when the carbon−nitrogen bond is being cleaved, in contrast with the previously proposed mechanism that involved the unlikely protonation of Asp120 by a diol group.[11] (ii) Arg121, which is important for catalysis by monozinc BcII,[48] is able to anchor Asp120 through a stable salt bridge during

(49) Deslongchamps, P. *Stereoelectronic Effects in Organic Chemistry*; Pergamon Press: New York, 1983.
(50) Lipscomb, W. N.; Sträter, N. *Chem. Rev.* **1996**, *96*, 2375−2433.
(51) Lovejoy, B.; Hassell, A. M.; Luther, M. A.; Weigl, D.; Jordan, S. R. *Biochemistry* **1994**, *33*, 8207−8215.
(52) Kleifeld, O.; Frenkel, A.; Martin, J. M. L.; Sagi, I. *Nat. Struct. Biol.* **2003**, *10*, 98−103.
(53) Rasia, R. M.; Vila, A. J. *J. Biol. Chem.* **2004**, *279* (25), 26046−26051.
(54) Felici, A.; Amicosante, G.; Oratore, A.; Strom, R.; Ledent, P.; Joris, B.; Fanuel, L.; Frere, J. M. *Biochem. J.* **1993**, *291*, 151−155.
(55) Chantalat, L.; Duee, E.; Galleni, M.; Frère, J. M.; Dideberg, O. *Protein Sci.* **2000**, *9*, 1402−1406.
(56) Seny, D.; Prosperi-Meys, C.; Bebrone, C.; Rossolini, G. M.; Page, M. I.; Noel, P.; Frère, J. M.; Galleni, M. *Biochem. J.* **2002**, *363*, 687−696.
(57) Garrity, J. M.; Carenbauer, A. L.; Herron, L. R.; Crowder, M. W. *J. Biol. Chem.* **2004**, *279* (2), 920−927.

the entire reaction. (iii) Cys221, which is conserved among B1 enzymes,[6,7] guides WAT toward the zinc ion, and orients the nucleophile through H-bond interactions.[20,55] (iv) The fully conserved His263 forms flexible H-bonds with Asp120, CEF, OH, and WAT during the reaction.[56]

Concluding Remarks

The present work allows us to propose a novel mechanism for β-lactam hydrolysis by monozinc BcII. The key feature of this mechanism is the expansion of the zinc coordination sphere by a water molecule in Step 1. This fact not only contributes to assist the nucleophilic attack, but also provides a proton donor adequately oriented for Step 2, and activated upon binding to the zinc ion. The conserved hydrogen bond network in the active site, defined by Asp120, Cys221, and His263, orients the nucleophile (as already proposed[17,25]), and guides this water molecule to the zinc ion after the substrate is bound.

Finally, considering the lack of an experimental structure of a substrate-enzyme complex for MBLs, this study provides a detailed theoretical model for the catalytic mechanism of this enzyme, which can be taken into account for the development of potential inhibitors. In particular, these inhibitors could possess a hydroxide moiety, which could mimic the presence of the ordered molecule.

Acknowledgment. We thank INFM and COFIN-MURST for financial support. LL thanks CONICET for a fellowship. A.J.V. is a staff member from CONICET and an International Research Scholar of the Howard Hughes Medical Institute. A.J.V. thanks the financial support from CONICET, ANPCyT, and HHMI.

Supporting Information Available: Additional figures and tables concerning QM/MM and classical simulations are reported. This material is available free of charge via the Internet at http://pubs.acs.org.

JA048071B